NJC

ARTICLE

# Taking the next step toward inert $Mn^{2+}$ complexes of open-chain ligands: the case of the rigid PhDTA‡ ligand†

Received 00th January 20xx,
Accepted 00th January 20xx

DOI: 10.1039/x0xx00000x

www.rsc.org/

Kristóf Póta,[a] Zoltán Garda,[a] Ferenc Krisztián Kálmán,[a] José Luis Barriada,[b] David Esteban-Gómez,[b] Carlos Platas-Iglesias,[b] Imre Tóth,[a] Ernő Brücher,[a] and Gyula Tircsó*[,a]

In line with our research to find inert Mn(II) complexes as contrast agents for Magnetic Resonance Imaging, we have studied the aromatic–ring rigidified EDTA-analogue *o*-phenylenediamine-*N*,*N*′,*N*′,*N*′-tetraacetic acid (PhDTA). The protonation constants ($K_i^H$) of PhDTA and stability constants of complexes formed between this open-chain ligand and several different biogenic metal ions ($Ca^{2+}$, $Mg^{2+}$, $Zn^{2+}$, $Cu^{2+}$, $Mn^{2+}$) have been determined in 0.15 M NaCl at 25 °C and compared with the values reported in the literature previously. Protonation constants are lower than those of the corresponding *cis*- and *trans*-CDTA complexes, which might be attributed to the electron withdrawing effect of the phenylene group. The lower total basicity of the ligand leads to lower stability constants for all the examined metal complexes. On the contrary, we have found that the conditional stability constants of $[Mn(PhDTA)]^{2-}$ and [Mn(*trans*-CDTA)]$^{2-}$ are approximately the same, as both complexes are 100% formed by pH 5 and their pM values are also comparable. The relaxivity of $[Mn(PhDTA)]^{2-}$ is nearly identical ($r_1$ = 3.72 $mM^{-1}s^{-1}$) to that determined previously for the [Mn(*trans*-CDTA)]$^{2-}$ complex ($r_1$ = 3.62 $mM^{-1}s^{-1}$), and its pH-dependence confirms the equilibrium model used for the fitting of the titration data. The results of kinetic studies of the metal exchange reactions reveal that the $[Mn(PhDTA)]^{2-}$ complex possesses a slightly better dissociation kinetics profile than [Mn(*trans*-CDTA)]$^{2-}$, which has been tested *in vivo* recently (including human injections). The half-life of the dissociation of the complex near to physiological pH at 25 °C is 19 hours. By using the rate constant calculated for the dissociation (pH=7.4, $c_{Cu2+}$=10 μM) and the half-life of excretion (1.6 hour), the ratio of the dissociated complex is estimated to represent 8% of the injected dose. DFT studies reveal that the metal coordination environment of $[Mn(PhDTA)]^{2-}$ is very similar to that of $[Mn(EDTA)]^{2-}$, both containing an inner-sphere water molecule. Cyclic voltammetry studies indicate that $[Mn(PhDTA)]^{2-}$ is slightly more resistant towards oxidation to the $Mn^{3+}$ complex than the EDTA analogue.

## Introduction

The effectiveness of $Gd^{3+}$-based contrast agents (CAs) used in Magnetic Resonance Imaging (MRI) examinations, such as Magnevist® or Dotarem®, is undisputable.[1] However the toxicity of the free $Gd^{3+}$ ion is high ($LD_{50}$ = 0.2-0.5 mmol/kg), and has been related to the development of Nephrogenic Systemic Fibrosis (NSF) by patients with reduced renal acute functions (e.g. chronic kidney disease) after administration of CAs.[2] Because of these toxicity problems, there is a growing interest in the development of new, less toxic complexes containing biogenic metal ions which are likely better tolerated by living organisms. Some transition metal ions, which possess lower electron spin than $Gd^{3+}$, can be used as the central core of a potential imaging agent. Such ions are for example high spin $Mn^{2+}$ ($d^5$),[3] $Fe^{3+}$ ($d^5$),[4] $Co^{2+}$ ($d^7$)[5] or $Ni^{2+}$ ($d^8$).[6]

In the case of the $Mn^{2+}$ ion, oxidation to $Mn^{3+}$ caused by oxygen may lead to a drastic decrease of the paramagnetic effect. Thus, the redox potential of $Mn^{2+}/Mn^{3+}$ system has to be raised above +0.8 V by means of a suitable chelating ligand to obtain a contrast agent that is not sensitive to the oxidative conditions. On the other hand, the complexes undergoing oxidation in biological conditions may also be valuable for MRI imaging as redox-activated CAs, as it was demonstrated by Aime[7] and more recently by Caravan and co-workers.[8] The thermodynamic stability and kinetic inertness of the $Mn^{2+}$ complexes are generally lower compared to the $Gd^{3+}$ complexes. In this respect, to develop $Mn^{2+}$ complexes for

[a] Department of Inorganic and Analytical Chemistry, Faculty of Science and Technology, University of Debrecen, Egyetem tér 1, H-4032 Debrecen, Hungary
E-mail address: gyula.tircso@science.unideb.hu
[b] Centro de Investigaciones Científicas Avanzadas (CICA), Departamento de Química, Universidade da Coruña, Campus da Zapateira-Rúa da Fraga 10, A Coruña, Spain

† Electronic Supplementary Information (ESI) available: Structures of the ligands mentioned in the text, cyclic voltammogram of $[Mn(EDTA)]^{2-}$, bond distances of the metal coordination environment and optimised Cartesian coordinates obtained with DFT calculations.
‡ PhDTA = o-phenylenediamine-*N*,*N*,*N*',*N*'-tetraacetic acid

This paper is dedicated to professors Carlos F. G. C. Geraldes and Lothar Helm on the occasion of their retirement.

application as CAs is a great challenge, because it requires a good balance between the thermodynamic stability, relaxation and kinetic requirements, which are all crucial for *in vivo* MRI applications. There is only one commercially available (although already withdrawn from the European markets) non-$Gd^{3+}$ based contrast agent, $[Mn(DPDP)]^{4-}$ (Mangafodipir, Teslascan®), which is applied in MRI examinations of liver.[9] The human body possesses mechanisms to eliminate the excess of $Mn^{2+}$, but this works only in a limited concentration range (beyond that range it also possesses toxic effects with symptoms resembling Parkinson's disease).[10]

The properties of $Mn^{2+}$ complexes formed with macrocyclic ligands (mostly derivatives of 9-aneN3, 12-aneN4, and pyridine containing macrocycles 12-PyaneN4, 15-PyaneN5 and 15-PyaneN3O2) synthesized and studied in the past 7-8 years predominantly by Éva Tóth and co-workers, see Figure S1) are also far from being optimal.[11-15] For instance $Mn^{2+}$ complexes of macrocyclic ligands, such as NOTA and DOTA, possess high thermodynamic stability and suitable kinetic inertness for *in vivo* applications. However, the relaxivity (relaxation enhancement spurred by the presence of 1 mM paramagnetic substance) of these complexes is low because of the lack of the inner-sphere water molecule(s). On the other hand, coordinated water molecule(s) are observed in the complexes formed with ligands of lower denticity (e.g. ONO2A, NO2A, PC1A or PC1P). However, the decrease in the number of metal binding sites offered by the ligand affects negatively the kinetic inertness and the stability of the $Mn^{2+}$ chelates. An acceptable balance of physicochemical properties (stability, redox potential, inertness and relaxivity of $Mn^{2+}$ complexes) was found for *cis*-DO2A[16] and its derivatives,[17] opening a passable avenue to $Mn^{2+}$-based MRI CAs. The $Mn^{2+}$ complexes formed with linear ligands have almost the same thermodynamic stability as the corresponding macrocyclic ones, but their kinetic inertness are several orders of magnitude lower.[12,13] For instance, while the $[Gd(DTPA)]^{2-}$ complex presents a half-life of 33 hours at pH 5, the dissociation of $[Mn(DTPA)]^{3-}$ is so fast at this pH that prevents the determination of the dissociation rate even with the stopped-flow technique (with a dead time of 8 ms).[14] At the same time, linear ligands represent some advantages over the macrocyclic ones, for instance because their synthesis is less challenging. Moreover, careful ligand design can supply candidates with improved stability,[18] and relaxivity,[19] owing to the planned interaction of the complexes with biomolecules such as HSA,[19-21] or even $Mn^{2+}$-based responsive probes relying on the use of bifunctional ligands.[22] Among the $Mn^{2+}$ complexes studied so far $[Mn(trans\text{-}CDTA)]^{2-}$ and related *trans*-CDTA derivatives (e.g. PyC3A) show by far the best kinetic parameters.[22-25] More recently, these complexes were successfully tested *in vivo* in mice, in dogs and surprisingly even in human studies confirming their applicability.[26]

The objective of this study is to determine the stability constants of $[M(PhDTA)]^{2-}$ complexes and compare them with the stabilities of the complexes formed with the structurally-related EDTA, *cis*- and *trans*-CDTA ligands (Scheme 1). The PhDTA ligand has an even more rigid structure than CDTA due to the presence of an *ortho*-phenylenediamine unit in the molecule. In the $Mn^{2+}$ complexes of the *cis*- and *trans*-CDTA ligands the two N atoms of the iminodiacetate groups define N-C-C-N angles of ~50º,[27] while the unsaturated nature of the phenyl unit of PhDTA forces a planar N-C-C-N entity. As a result, the structure of the $Mn^{2+}$ complex of PhDTA is expected to be somewhat different to that of $[Mn(trans\text{-}CDTA)]^{2-}$, which in turn may lead to differences between the thermodynamic and kinetic properties of the two complexes. We do not expect a drastic change in relaxivity because of the presence of a coordinated water molecule and the identical overall charge of both complexes.[28] The thermodynamic properties of the PhDTA ligand and several of its metal complexes were studied in the 1980's and 1990's, but because of the differences in terms of the applied procedures (e.g. calorimetry, extraction method, etc.) and ionic strengths (1.0 M $NaClO_4$), as well as due to the large differences in the reported stability data (for $[Cu(PhDTA)]^{2-}$ a difference of 10 log units can be found in the literature),[29-33] we decided to determine these values using an ionic strength close to the physiological conditions (0.15 M NaCl). Therefore, we synthesized the PhDTA ligand and redetermined the stability constants of the $Mn^{2+}$ complex and those with other biogenic metal ions. Furthermore, we investigated the dissociation kinetics, relaxometric and electrochemical properties of the $[Mn(PhDTA)]^{2-}$ complex. Finally, the structure of the $[Mn(PhDTA)]^{2-}$ complex in solution was studied by using DFT calculations.

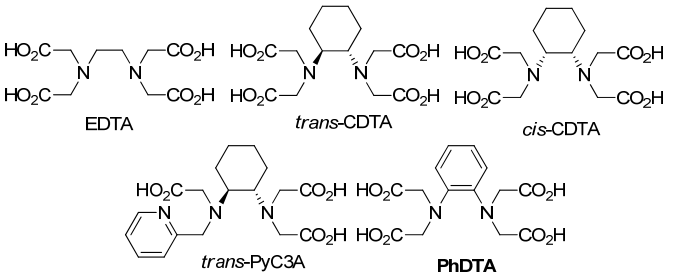


**Scheme 1.** Ligands discussed in the present work.

## Results and discussion

### Equilibrium and Relaxometric Studies

The protonation constants of the PhDTA ligand must be determined to subsequently measure the stability constant of the $[Mn(PhDTA)]^{2-}$ complex. For this purpose direct pH-potentiometric titrations have been carried out. During these studies it is essential to choose an appropriate ionic strength because the ions used to adjust the ionic strength interact with both the ligand and metal ion. We have chosen a 0.15 M NaCl ionic strength to model the NaCl background present in the body fluids. The protonation constants obtained by potentiometry are shown in Table 1 along with the ones determined previously using different ionic strengths[30,31,33] and the corresponding values of the EDTA and *cis*- or *trans*-CDTA chelators.[27] The comparison of the constants excels that the log $K_i^H$ values of PhDTA are lower than those of CDTA

 

ligands, with the total basicity of PhDTA being four orders of magnitude lower. In these ligands (EDTA, *cis*- and *trans*-CDTA and PhDTA) the first two protonation processes are attributed to the two amine nitrogen atoms, while the protonations occurring at acidic pH correspond to the acetate groups. The considerable difference between the first two protonation constants can be ascribed to the lower basicity of anilines compared to aliphatic amines, which is the result of delocalization of the nitrogen atom's lone pair onto the aromatic unit. The 3$^{rd}$ and the 4$^{th}$ protonation constant of the PhDTA chelator can be assigned to the protonation of carboboxylate pendants while 5$^{th}$ and 6$^{th}$ protonation cannot be measured by pH-potentiometry. This suggests that these protons are very acidic and dissociate easily in aqueous media, similarly to the protons of strong acids. By comparing the protonation constants with the previously reported ones, we did not found significant deviations. The small differences may arise from the applied ionic strength and less likely from different measurement techniques.

In view of the protonation constants determined here, the stability and protonation constants of PhDTA complexes formed with biogenic metal ions are not expected to deviate notably from the literature data. The acquired stability constant values are also shown in Table 1, where the data reported previously for PhDTA, EDTA and CDTAs are provided for comparison. As expected from the total basicity values, the stability constants of the PhDTA complexes are significantly lower compared to the EDTA and CDTA analogues. In the cases of $Mg^{2+}$, $Ca^{2+}$ and $Mn^{2+}$ the stability constants drop by 3-4 orders of magnitude, but the decrease of the stability constants of the PhDTA complexes with $Zn^{2+}$ and $Cu^{2+}$ exceeds 6 orders of magnitude. However, the species distribution curves of $[Mn(PhDTA)]^{2-}$ and $[Mn(trans\text{-}CDTA)]^{2-}$ complexes (Figure 1) indicate that complex formation begins at pH 2.0 and ends at around pH 5.0 in both systems, which means that their apparent stability is nearly the same. This is supported by calculating and comparing the pMn values at pH 7.4 with 10 µM ligand and 10 µM $Mn^{2+}$ concentrations (8.36 for $[Mn(PhDTA)]^{2-}$ and 8.68 $[Mn(trans\text{-}CDTA)]^{2-}$).[15] In the case of $Mg^{2+}$, $Ca^{2+}$, $Mn^{2+}$, $Zn^{2+}$ and $Cu^{2+}$ ions the formation of ML, mono- (MHL) and diprotonated ($MH_2L$) complex species was established. Potentiometric studies have also been carried out with 2:1 metal-ligand ratios with $Mn^{2+}$, $Zn^{2+}$ and $Cu^{2+}$ to investigate the formation of dinuclear complexes. Both $Zn^{2+}$ and $Cu^{2+}$ form this kind of complexes with PhDTA, including protonated dinuclear species, though they possess low stability. The stability constant of the $[Cu(PhDTA)]^{2-}$ complex could not be determined by using solely the pH-potentiometric data, as the $Cu^{2+}$ ion is mostly in complexed form (~85%) even near pH = 1 (Figure 2). Therefore, the stability of this complex was assessed by using a combination of the UV-vis spectrophotometric method (applicable to very acidic samples) and pH-potentiometry titration data obtained at higher pH. The absorption spectra of the $[Cu(PhDTA)]^{2-}$ complex as a function of $H^+$ ion concentration are shown in Figure 3. In line with the equilibrium data obtained for the other metal ions studied, the stability constant of the $[Cu(PhDTA)]^{2-}$ complex is smaller than the value of the $Cu^{2+}$ complexes of EDTA derivatives determined under identical conditions. On the other hand the stability constant determined in our study is in excellent agreement with the value determined previously by M. Tanaka and co-workers,[32] indicating that the stability constants published recently for $M^{2+}$ complexes by T. Zhang and co-workers[33] are not really reliable.

The pH dependence of the relaxivity of $[Mn(PhDTA)]^{2-}$ was studied to acquire information about the relaxivity of the complex ($r_{1p}$) on one hand, and to support the equilibrium model used in the analysis of the pH-potentiometric titrations on the other hand. As shown in Figure 4, the formation of a monoprotonated complex does not cause a considerable change in the relaxivity (only 0.3 – 0.5 $mM^{-1}s^{-1}$ units). The dissociation of the complex starts at pH < 3.5 leading to significant increase in the relaxivity because of the formation of $[Mn(H_2O)_6]^{2+}$ (characterized by a $r_{1p}$ value of 7.92 $mM^{-1}s^{-1}$ at 20 MHz and 25 °C). The measured relaxivity values remain constant in the pH range of 5-10, and then slightly decrease above pH 10. This can be interpreted by the oxidation of manganese upon the dissociation of a mixed hydroxo complex. The mixed hydroxo complex has not been studied because atmospheric oxygen oxidizes $Mn^{2+}$ under the applied conditions. The relaxivity of the $[Mn(PhDTA)]^{2-}$ complex is $r_{1p}$ = 3.72 $mM^{-1}s^{-1}$ (between pH 5-10), which is very similar to that

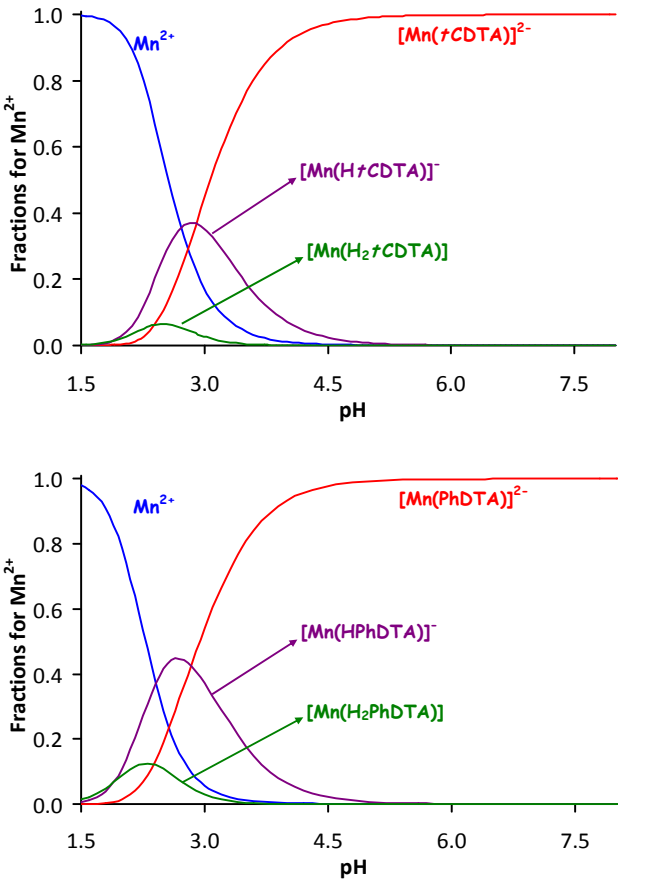


**Figure 1.** Concentration distribution curves calculated for $[Mn(PhDTA)]^{2-}$ and $[Mn(trans\text{-}CDTA)]^{2-}$ complexes ($c_{Mn2+} = c_L$ = 0.001 M).

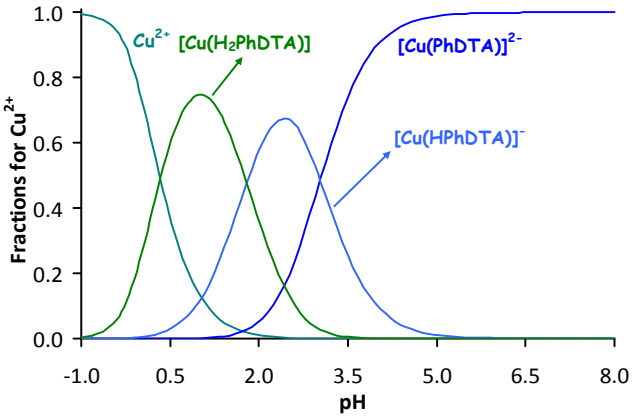


**Figure 2.** The species distribution curve calculated for the $[Cu(PhDTA)]^{2-}$ complex by using the stability constants determined via combined UV-vis and pH-potentiometric titration data ($c_{Cu2+} = c_L = 0.001$ M)).

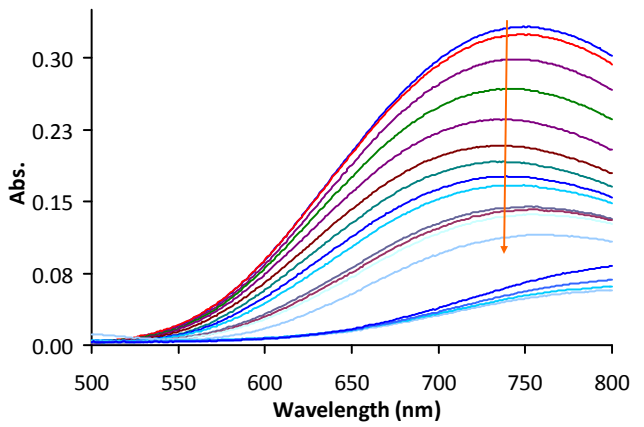


**Figure 3.** Absorption spectra of the $[Cu(PhDTA)]^{2-}$ complex ($[Cu^{2+}]_{tot} = [PhDTA]_{tot} = 4\times10^{-3}$ M) recorded at different pH: 4.96, 4.06, 3.43, 2.99, 2.59, 2.30, 2.00, 1.71, 1.51, 1,30, 1.15, 1,0 and 0.7. The lower spectra correspond to the $Cu^{2+}$ ion in solution at the same concentration and pH=1.0, 0.7, 0.3, and 0 (pH=-log[$H^+$]).

**Table 1**. Protonation and stability constants of the EDTA, *cis*- and *trans*-CDTA and PhDTA ligands and their complexes formed with $Ca^{2+}$, $Mg^{2+}$, $Mn^{2+}$, $Cu^{2+}$ and $Zn^{2+}$ ions ($I$ = 0.15 M NaCl, $T$ = 25 °C).[a]

| | | EDTA[a] | *trans*-CDTA[a] | *cis*-CDTA[c] | PhDTAD[d] | PhDTA |
|---|---|---|---|---|---|---|
| $H^+$ | log $K_1^H$ | 9.17[b] | 9.36[b] | 11.00 | 6.41; 5.95[e] | 6.66(5) |
| | log $K_2^H$ | 5.99[b] | 5.95[b] | 5.20 | 4.61; 3.70[e] | 4.85(6) |
| | log $K_3^H$ | 2.73[b] | 3.62[b] | 3.41 | 3.53; 2.79[e] | 3.53(7) |
| | log $K_4^H$ | 2.01[b] | 2.57[b] | 2.30 | 3.00; –[e] | 3.32(6) |
| | log $K_5^H$ | 1.38[b] | 1.49[b] | 1.41 | – | – |
| | $\sum$ log $K_i^H$ | 21.28[b] | 22.99[b] | 23.32 | 17.55; 12.44[e] | 18.36 |
| $Mg^{2+}$ | log $K_{ML}$ | 7.61 | 9.14 | 9.01 | 6.48[f]; 10.41[e] | 6.94(3) |
| | log $K_{MHL}$ | – | 3.53 | 4.72 | 2.7[f] | 3.78(6) |
| $Ca^{2+}$ | log $K_{ML}$ | 9.53 | 10.23 | 9.65 | 8.27[f]; 11.25[e] | 8.79(2) |
| | log $K_{MHL}$ | 2.92 | 3.53 | 4.55 | 3.0[f] | 3.38(3) |
| $Mn^{2+}$ | log $K_{MnL}$ | 12.46[b] | 14.32[b] | 14.19 | 11.37 | 11.79(2) |
| | log $K_{MnHL}$ | 2.95[b] | 2.90[b] | 2.85 | 2.29 | 2.84(2) |
| | log $K_{MnH2L}$ | –[b] | 1.89[b] | – | 1.70 | 1.91(5) |
| | pMn[g] | 7.83 | 8.68 | 7.82 | 8.16 | 8.38 |
| $Cu^{2+}$ | log $K_{ML}$ | 19.02[h] | 19.78[h] | 18.3(1)[h] | 15.21[h]; 24.84[f] | 15.21(6)[h] |
| | log $K_{MHL}$ | 3.15 | 2.91 | 3.65 | 3.04 | 3.35(1) |
| | log $K_{MH2L}$ | 2.04 | 1.10 | – | 1.80 | 2.18(1) |
| | log $K_{M2L}$ | – | – | – | – | 2.75(2) |
| $Zn^{2+}$ | log $K_{ML}$ | 15.92 | 16.75 | 17.06 | 12.89; 17.99[f] | 13.03(3) |
| | log $K_{MHL}$ | 3.23 | 2.57 | 2.76 | 2.96 | 3.56(2) |
| | log $K_{MH2L}$ | 1.50 | – | – | 1.30 | 1.90(3) |
| | log $K_{M2L}$ | – | – | – | – | 2.69(7) |

[a] 0.15 M NaCl, 25°C from the diploma work of Veronika Józsa, 2015, University of Debrecen, Debrecen, Hungary; [b] Ref. 23.; [c] Ref. 27; [d] Ref. 32; [e] Ref. 33; [f] Ref. 31; [g] Calculated by using $c_{Mn}=c_{Lig}$=0.01 mM at pH=7.4 according to Ref. 15.; [h] Determined by simultaneous fitting of the UV-vis and pH-potentiometic data.

**Table 2**. Rate and stability constants characterizing the dissociation of the $[Mn(EDTA)]^{2-}$, $[Mn(cis\text{-}CDTA)]^{2-}$, $[Mn(trans\text{-}CDTA)]^{2-}$ and $[Mn(PhDTA)]^{2-}$ complexes ($I$ = 0.15 M NaCl, $T$ = 25 °C).

| | EDTA[a, b] | *cis*-CDTA[c] | *trans*-CDTA[a, b] | PhDTA |
|---|---|---|---|---|
| $k_1$ ($M^{-1}s^{-1}$) | $5.2\times10^4$ | $1.02\times10^5$ | $4.0\times10^2$ | $(2.01\pm0.04)\times10^2$ |
| $k_2$ ($M^{-2}s^{-1}$) | $2.3\times10^8$ | – | – | $(4.9\pm0.3)\times10^5$ |
| $k_3$ ($M^{-1}s^{-1}$) | 45 | – | – | 0.21±0.01 |
| $K_{MnLCu}$ | – | 79 | 79 | 27±4 |
| log $K_H$ | 2.65[d] | 2.85[d] | 2.90[d] | 2.84[d] |
| $t_{1/2}$ (h)[e] | 0.076 | 0.47 | 12.3 | 19.1 |

[a] Ref. 23. [b] For for $[Mn(edta)]^{2-}$ $k_3 = 3.0\times10^{-1}$ $M^{-1}s^{-1}$, $k_4$ = ~$4.8\times10^1$ $M^{-2}s^{-1}$ and log $K_{MnHL}$=3.10 while $[Mn(trans\text{-}cdta)]^{2-}$ $k_1 = 3.2\times10^2$ $M^{-1}s^{-1}$ and $t_{1/2}$ = 15 h were found in Ref. 35. [c] Ref. 27. [d] Determined by pH-potentiometry and fixed in the data fitting. [e] Calculated at pH = 7.4 in the presence of $c_{Cu2+}=1\times10^{-5}$ M.

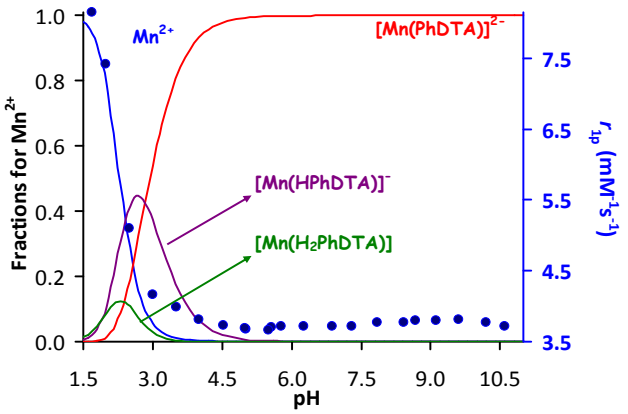


**Figure 4.** The speciation distribution of $[Mn(PhDTA)]^{2-}$ complex with the pH dependence of its relaxivity ($I$ = 0.15 M NaCl, $T$ = 25 °C, 20 MHz).

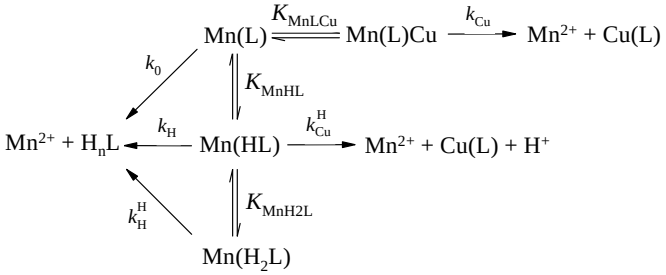


**Scheme 2.** Reaction mechanisms for the dissociation of the $[Mn(PhDTA)]^{2-}$ complex.

determined previously for the $[Mn(trans\text{-}CDTA)]^{2-}$ complex.[23,27] Thus, we conclude that the replacement of the cyclohexanediamine unit by ortho-phenylenediamine bridge does not affect significantly the relaxivity of the $Mn^{2+}$ complexes.

### Dissociation kinetics of the $[Mn(PhDTA)]^{2-}$ complex

Since $Mn^{2+}$ is a biogenic metal ion, its toxicity is considerably lower than that of $Gd^{3+}$. Nevertheless $Mn^{2+}$ is also harmful in large doses and causes symptoms similar to the ones associated with Alzheimer's disease.[34] Thus, our goal is to prepare $Mn^{2+}$-based contrast agents that do not dissociate *in vivo* to avoid potential toxicity issues. With an aim of gaining information about its inertness the rates of the exchange reactions of $[Mn(PhDTA)]^{2-}$ have been studied in the presence of $Cu^{2+}$. The kinetic experiments have been conducted in the pH range of 3.6 – 5.2 with the use of $Cu^{2+}$ as exchanging metal ion. These transmetallation reactions are slow enough in the mentioned pH range to allow for measurements with conventional spectrophotometric methods. The studied exchange reactions can be delineated as follows:

$$[Mn(PhDTA)]^{2-} + Cu^{2+} \rightleftharpoons [Cu(PhDTA)]^{2-} + Mn^{2+}$$

For the metal exchange reactions, the concentration of $Cu^{2+}$ was 10 to 40 times higher than the concentration of the complex to assure pseudo-first-order conditions. Fitting the acquired time-absorbance curves to the equation for a first order reaction gave the pseudo-first-order rate constant ($k_{obs}$) for each reaction. The $H^+$ concentration dependence of the dissociation rates are shown in Figure 5. It is obvious that the reaction rates show a second order dependence on proton concentration. Furthermore, the experiments performed using different concentrations of $Cu^{2+}$ indicate that the role of the metal ion is not negligible, i.e. the dissociation can be realized through a heterodinuclear complex. The acquired rate constants increase with the rise of $H^+$ concentration and change by varying $Cu^{2+}$ concentration. Accordingly, the reaction can occur both with the attack of protons and the exchanging metal ion. However the effect of the exchanging metal ion on the reaction rates depend strongly on pH. While the increase of the $Cu^{2+}$ concentration leads to lower reaction rates in the more acidic samples, at higher pH it leads to higher reaction rates (Figure 6). The explanation for this behavior might be that the two reaction pathways (the proton assisted and the metal ion assisted paths) are in competition with each other. For the dissociation of the complex in the presence of $Cu^{2+}$ the general reaction scheme shown in Scheme 2 can be established. Taking into account the different reaction pathways (characterized by the rate coefficients $k_0$, $k_H$, $k_H^H$, $k_{Cu}$, $k_{Cu}^H$), the protonation constants and stability constants of the complexes ($K_{MnHL}$, $K_{MnH_2L}$ and $K_{MnLCu}$), the pseudo-first-order rate constant ($k_{obs}$) can be expressed by eqn. 1, where $K_{MnHL}=[Mn(HL)]/([Mn(L)][H^+])$, $K_{MnH_2L}=[Mn(H_2L)]/([Mn(HL)][H^+])$, $K_{MnLCu}=[Mn(L)Cu]/([Mn(L)][Cu^{2+}])$, $k_1=k_H\cdot K_{MnHL}$, $k_2=k_H^H\cdot K_{MnHL}\cdot K_{MnH2L}$, $k_3=k_{Cu}\cdot K_{MnLCu}$ and $k_4=k_{Cu}^H\cdot K_{MnHL}$.[35]

$$k_{obs} = \frac{k_0 + k_1[H^+] + k_2[H^+]^2 + k_3[Cu^{2+}] + k_4[Cu^{2+}][H^+]}{1 + K_{MnHL}[H^+] + K_{MnHL}K_{MnH_2L}[H^+]^2 + K_{MnLCu}[Cu^{2+}]} \quad (1)$$

Initial attempts to fit the experimental data to eqn. 1 evidenced that beside two proton-assisted pathways (characterized by $k_1$ and $k_2$) the attack of the metal ion with the formation of a dinuclear complex also affects the dissociation reaction. The $k_4$ rate constant gave a negative value during the fitting thus the path was neglected. Taking into consideration the pathways mentioned above, the pseudo-first order rate constants of the exchange reaction were analyzed using the following simplified expression (eqn. 2):

$$k_{obs} = \frac{k_1[H^+] + k_2[H^+]^2 + k_3[Cu^{2+}]}{1 + K_{MnHL}[H^+] + K_{MnLCu}[Cu^{2+}]} \quad (2)$$

The rate and stability constants obtained by fitting the $k_{obs}$ values are compared with the data acquired for the $[Mn(EDTA)]^{2-}$, $[Mn(cis\text{-}CDTA)]^{2-}$ and $[Mn(trans\text{-}CDTA)]^{2-}$ complexes in Table2. The results show that, in the case of the

*trans*-CDTA complex, the partial decoordination of the ligand from $Mn^{2+}$ and coordination to $Cu^{2+}$ is a slow process, which results in the formation of a quite stable dinuclear intermediate (a so-called "dead-end" complex). The formation of the dinuclear species slows down the reaction by decreasing the contribution of the proton assisted pathway. On the contrary, the dinuclear complex formed with PhDTA possesses a "Janus-face" nature in affecting the rate of the reaction depending on $H^+$ concentration. This can be explained by a positive contribution of the metal-assisted pathway to the overall exchange reaction above pH 4.6 (Fig 6), while at pH below pH 4.3 the slower metal-assisted dissociation competes with the proton assisted pathway, thus lowering the pseudo-first rate constants. It is obvious from the data shown in Table 2 that the rate of the proton assisted dissociation in the case of $[Mn(PhDTA)]^{2-}$ is half of that of $[Mn(trans\text{-}CDTA)]^{2-}$, which is reassuring with respect of a potential application of the complex. The half-life of dissociation of the $Mn^{2+}$ complexes have been calculated using the first order rate constants at pH 7.4 and 25 °C ($c_{Cu^{2+}}$=0.01 mM). The results indicate that the $[Mn(PhDTA)]^{2-}$ complex presents the highest inertness with respect to complex dissociation among the four complexes ($t_{1/2,[Mn(PhDTA)]^{2-}}$= 19.1 h considering seven times the depletion and not considering the reformation of the complex, and $t_{1/2,[Mn(trans\text{-}CDTA)]^{2-}}$= 12 h) while the dissociation of the $[Mn(EDTA)]^{2-}$ and $[Mn(cis\text{-}CDTA)]^{2-}$ complexes is complete within few minutes under these conditions). Considering the typical excretion time of low molecular weight contrast agents ($t_{1/2}$ = 1.6 h), the $[Mn(PhDTA)]^{2-}$ complex appears to be a good candidate for *in vivo* experiments.

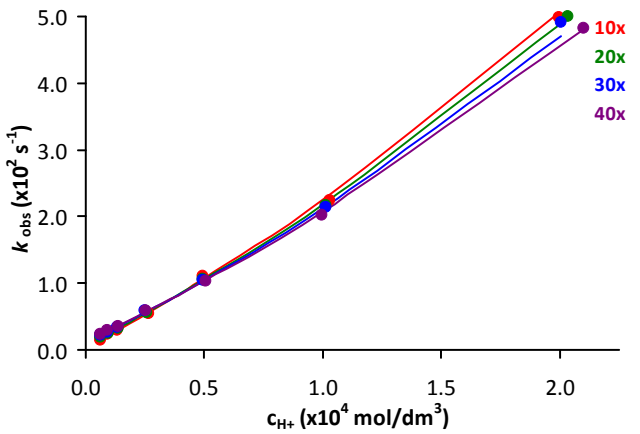


**Figure 5.** Dissociation rates ($k_{obs}$) of the $[Mn(PhDTA)]^{2-}$ complex plotted as a function of $H^+$ ion concentration ($I$ = 0.15 M NaCl, $T$ = 25 °C). The colors represent different $Cu^{2+}$ ion concentration as follows: 2 mM (red), 4 mM (green), 6 mM (blue) and 8 mM (purple).

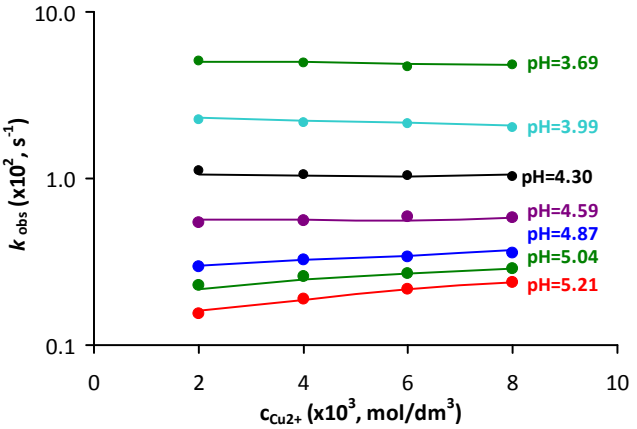


**Figure 6.** Dissociation rates ($k_{obs}$) of the $[Mn(PhDTA)]^{2-}$ complex plotted as a function of $Cu^{2+}$ ion concentration ($I$ = 0.15 M NaCl, $T$ = 25 °C).

## DFT calculations

DFT calculations were carried out to gain insight into the structure of the $[Mn(PhDTA)]^{2-}$ complex in solution. Geometry optimizations were performed on the $[Mn(PhDTA)(H_2O)]^{2-}\cdot 2H_2O$ system, as the explicit inclusion of two second-sphere water molecules involved in hydrogen-bonding interactions with the coordinated water molecule are required for an accurate calculations of $Mn\text{-}O_{water}$ distances and scalar hyperfine coupling constants at the $^{17}O$ nucleus of the coordinated water molecule.[36] The optimized geometry (Fig 7) calculated at the M062X/TZVP level shows a very good agreement with the X-ray crystallographic data reported by Tanaka et al.[37] The calculated bond distances deviate from the experimental ones by < 0.036 Å (Table S1, ESI†). A comparison of the structure obtained for $[Mn(PhDTA)(H_2O)]^{2-}\cdot 2H_2O$ and that calculated for $[Mn(EDTA)(H_2O)]^{2-}\cdot 2H_2O$ using the same methodology reveals that the average Mn-N distance is somewhat shorter in the EDTA complex (2.411 Å) than in the PhDTA one (2.440 Å). An opposite situation is observed for the $Mn\text{-}O_{carboxylate}$ distances, which show average values of 2.243 and 2.215 Å for $[Mn(EDTA)(H_2O)]^{2-}\cdot 2H_2O$ and $[Mn(PhDTA)(H_2O)]^{2-}\cdot 2H_2O$, respectively. The shorter $Mn\text{-}O_{carboxylate}$ distances observed for $[Mn(PhDTA)(H_2O)]^{2-}\cdot$are likely responsible for the higher kinetic inertness of this complex with respect to the EDTA derivative, as the proton-assisted dissociation pathway likely involves decoordination of a protonated acetate group, while the metal-assisted mechanism also requires decoordination of acetate groups to form a dinuclear intermediate.

The $Mn\text{-}O_{water}$ distance calculated for $[Mn(PhDTA)(H_2O)]^{2-}\cdot$(2.273 Å) is similar to that observed in the solid state (2.242 Å)[37] and only slightly longer than the value calculated for $[Mn(EDTA)(H_2O)]^{2-}\cdot 2H_2O$ (2.251 Å). The $^{17}O$ hyperfine coupling constant obtained using DFT ($A_O/\hbar$ = -42.6×10$^6$ rad s$^{-1}$) is in excellent agreement with the experimental value reported by Hunt ($A_O/\hbar$ = -38.0×10$^6$ rad s$^{-1}$),[28] which indicates that our calculations provide an adequate description of the spin density distribution on the $Mn\text{-}O_{water}$ bond.

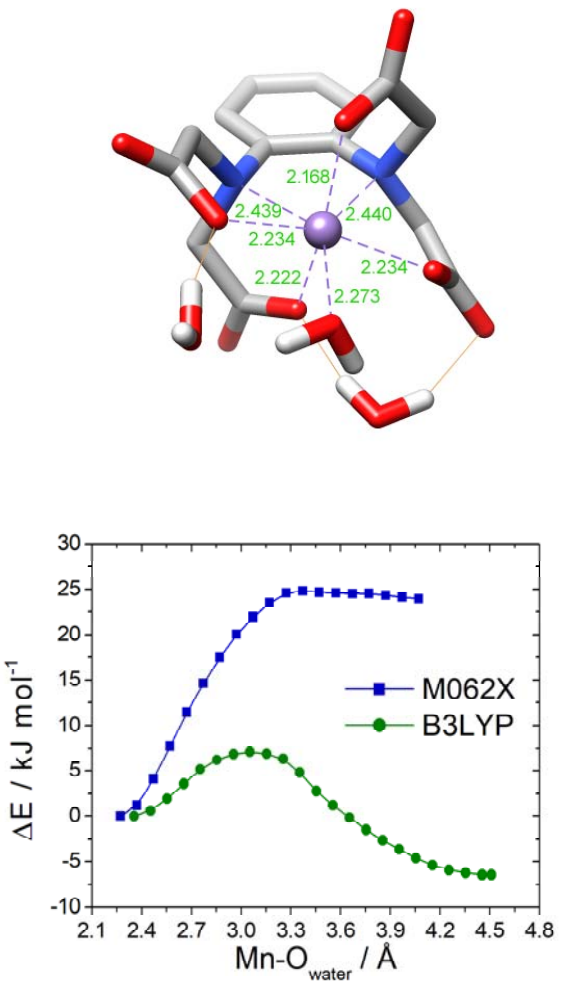


**Figure 7.** Top: Structure of the $[Mn(PhDTA)(H_2O)]^{2-}\cdot 2H_2O$ system obtained using DFT calculations at the M062X/TZVP level. Bottom: Relaxed potential energy surface scans calculated for $[Mn(PhDTA)(H_2O)]^{2-}\cdot 2H_2O$ using different functionals.

The experimental determination of the number of water molecules coordinated to $Mn^{2+}$ in potential MRI contrast agents remains a difficult task. Caravan et al.[38] proposed a method relying on the analysis of the temperature dependence of the transverse $^{17}O$ NMR relaxation rates. This method can only be applied to systems undergoing a changeover from a slow exchange regime at low temperature to a fast exchange regime at high temperature. As a consequence, the hydration number of complexes whose transverse relaxation rates are in the fast exchange regime in the whole accessible temperature range cannot be estimated using this methodology. Thus, we wanted to explore whether our DFT calculations could provide information on the number of coordinated water molecules. For this purpose, we explored the potential energy surface (PES) of the $[Mn(EDTA)(H_2O)]^{2-}\cdot 2H_2O$ and $[Mn(PhDTA)(H_2O)]^{2-}\cdot 2H_2O$ systems by increasing the $Mn\text{-}O_{water}$ distance (Fig 7, see also Fig S2, ESI†). These relaxed PES scans provided the six-coordinate $[Mn(EDTA)]^{2-}\cdot 3H_2O$ and $[Mn(PhDTA)]^{2-}\cdot 3H_2O$ structures, which turned out to be less stable than the seven-coordinate forms at the M062X/TZVP level, in line with the experimental evidence. However, the PES was found to differ considerably depending on the particular functional used. For instance the B3LYP functional stabilizes considerably the six-coordinated structures, which in the case of the PhDTA complex is the most stable form at the B3LYP/TZVP level. This is in line with our recent results that showed that M062X/TZVP calculations provided energy profiles for the water exchange reactions of $[Li(H_2O)_4]^+$ and $[Be(H_2O)_4]^{2+}$ in good agreement with the experiment, while B3LYP/TZVP calculations overstabilized a lower coordination numbers.[39] While an exhaustive evaluation of different functionals is beyond the scope of the present study, the results obtained here suggest that M062X/TZVP calculations may be useful in predicting hydration numbers of $Mn^{2+}$ complexes relevant as MRI contrast agents.

### Electrochemical measurements

The redox stability of the $[Mn(PhDTA)]^{2-}$ complex was investigated using cyclic voltammetry experiments in aqueous 0.15 M NaCl. The cyclic voltammograms obtained using different scan rates are characteristic of an irreversible system. The cyclic voltammogram recorded at a scan rate of 50 mV/s showed an oxidation peak at $E_{ox}$ = +813 mV and a reduction peak at $E_{red}$ = +552 mV ($\Delta E_{1/2}$ = 683 mV vs Ag/AgCl, Fig 8). The cyclic voltammogram obtained for $[Mn(EDTA)]^{2-}$ using the same conditions shows both the anodic ($E_{ox}$ = +769 mV) and cathodic ($E_{ox}$ = +510 mV) peaks shifted to lower potentials, which shows that PhDTA presents a lower ability to stabilize $Mn^{3+}$ compared to EDTA. This might be related to the harder nature of the amine nitrogen atoms of EDTA compared to the aniline donor atoms of PhDTA (according to Pearson's HSAB principle). This may be also related to the differences in the geometries as evidenced for $[Mn(PhDTA)]^{2-}$ by X-ray crystallography when compared with that of the [Mn(*trans*-CDTA)]$^{2-}$ complex,[37, 40] as any axial distortion of the Mn(II) coordination environment should favour Mn(III) over Mn(II), thereby leading to a decrease in potential.[41, 42] The half-cell potential of $[Mn(EDTA)]^{2-}$ ($\Delta E_{1/2}$ = 640 mV vs Ag/AgCl, Figure S3, ESI†) is very similar to that reported by Caravan using 0.5 M $KNO_3$ as supporting electrolyte (633 mV).[8]

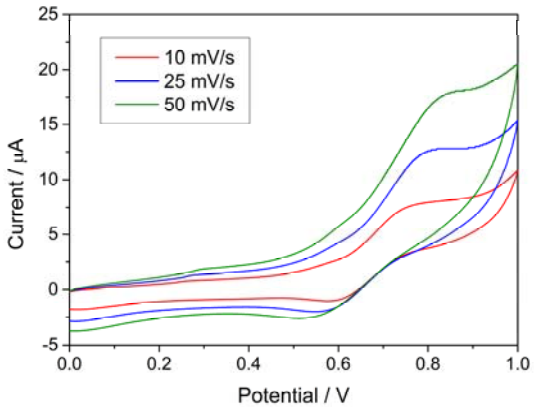


**Figure 8.** Cyclic voltammograms recorded using different scan rates for 3 mM $[Mn(PhDTA)]^{2-}$ (pH = 7.1, 0.15 NaCl, potentials reported vs Ag/AgCl).

## Conclusions

The replacement of the ethylenediamine bridging unit in EDTA by the ortho-phenylenediamine backbone to give PhDTA decreases the basicity of the ligand owing to the electron withdrawing effect of the aromatic unit, yet the PhDTA complexes formed with $Ca^{2+}$, $Mg^{2+}$, $Mn^{2+}$, $Cu^{2+}$ and $Zn^{2+}$ possess very similar conditional stabilities to those of the corresponding EDTA complexes. The kinetic studies approached by studying the metal exchange reactions occurring between the $Cu^{2+}$ ion and the $[Mn(PhDTA)]^{2-}$ complex revealed an improved inertness compared to $[Mn(trans\text{-}CDTA)]^{2-}$. The complex possesses a half-life of 19.1 hours at physiological pH and 25 °C, thus only about 8% of the injected amount is expected to dissociate in the body. It has to be emphasized however that at 37 °C the extent of the dissociation will likely be slightly higher, and thus further ligand design is needed to find even better ligand candidates for $Mn^{2+}$ ion complexation. DFT calculations confirmed that the $[Mn(PhDTA)]^{2-}$ complex possesses one metal bound water molecule (in agreement with the solid state structure of the complex published previously[37]). As a result, we found a relaxivity ($r_1$ = 3.72 $mM^{-1}s^{-1}$ at 20 MHz and 25 °C) very similar to those determined earlier for the $Mn^{2+}$ complexes formed with EDTA as well as *cis*- or *trans*-CDTA ligands (Table 3). The most important physicochemical parameters of the $[Mn(EDTA)]^{2-}$, $[Mn(cis\text{-}CDTA)]^{2-}$, $[Mn(trans\text{-}CDTA)]^{2-}$ and $[Mn(PhDTA)]^{2-}$ complexes are collected and compared in Table 3. As it can be seen form the data compared in Table 3 the *ortho*-phenylenediamine building block represents an attractive alternative to the *trans*-1,2-cyclohexanediamine unit when tailoring inert open-chain based $Mn^{2+}$ complexes for safe MRI applications.

**Table 3**. Rate and stability constants characterizing the dissociation of the $[Mn(EDTA)]^{2-}$, $[Mn(cis\text{-}CDTA)]^{2-}$, $[Mn(trans\text{-}CDTA)]^{2-}$ and $[Mn(PhDTA)]^{2-}$ complexes ($I$ = 0.15 M NaCl, $T$ = 25 °C).

| | EDTA[a] | *cis*-CDTA[b] | *trans*-CDTA[a] | PhDTA |
|---|---|---|---|---|
| log $K_{[Mn(L)]}$ | 12.46 | 14.19 | 14.32 | 11.79 |
| pMn[c] | 7.83 | 7.82 | 8.68 | 8.38 |
| $k_{ex}^{298}$ ($x10^7$ $s^{-1}$) | 41[d] | 22.5 | 14.0[e] | 35.0[f] |
| $r_{1p}^{298}$ ($mM^{-1}s^{-1}$)[g] | 3.20 | 3.85 | 3.62 | 3.72 |
| $t_{1/2}$ (h)[h] | 0.076 | 0.47 | 12.2 | 19.1 |

[a] Ref. 23; [b] Ref. 27; [c] pMn values were calculated at pH=7.4 by using 0.01 mM $Mn^{2+}$ and ligand concentration as suggested by É. Tóth and o-workers, Ref. 15; [d] From Ref.43; [e] From Ref. 44; [f] From Ref. 45; [g] at 25 °C and 20 MHz; [h] The half-lives (h) of dissociation were extrapolated to pH=7.4 by using 0.01 mM $Cu^{2+}$ ion concentration

## Experimental Section

### Synthesis

The ligand PhDTA was synthesized as shown in Scheme 3 using a slight modification of the previously published procedure.[33]

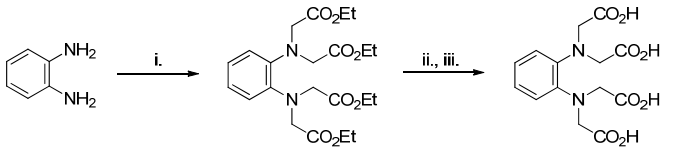


**Scheme 3.** Synthesis of PhDTA. Reagents and conditions: i) $BrCH_2COOEt$, DIPEA, NaI, MeCN; ii) NaOH, EtOH; iii) $HCl/H_2O$ and crystallization.

***ortho*-Phenylenediamine-*N,N,N',N'*-tetraacetate tetraethyl ester (1).** 1,2-Diaminobenzene (1.10 g, 10.2 mmol), ethyl-bromoacetate (6.70 mL,10.1 g, 60.5 mmol), sodium iodide (1.30 g, 8.67 mmol) and *N,N*-diisopropylethylamine (8.30 mL, 6.16 g, 47.7 mmol) were mixed in acetonitrile (10 mL) and the mixture was refluxed under $N_2$ atmosphere for 7 hours. After cooling to room temperature, the reaction mixture was evaporated under reduced pressure. Water (50 mL) was added to the residue and the mixture extracted with chloroform (3×40 mL). The combined organic extracts were dried with $Na_2SO_4$ and evaporated under reduced pressure resulting in a brown oil, which was purified with flash silica gel chromatography (petroleum ether:ethyl-acetate 10:1). Yield 2.90 g (62%).

***ortho*-Phenylenediamine-*N,N,N',N'*-tetraacetic acid (PhDTA).** The ethyl ester precursor **1** (2.90 g, 6.41 mmol) was dissolved in ethanol (40 mL) and NaOH (1.28 g, 32 mmol) dissolved in distilled water (5 mL) was added dropwise to the stirred reaction mixture. A white precipitate was formed and the mixture was refluxed for 18 hours. The white crystalline product was filtered with G3 filter crucible and dissolved in water (2-3 mL). The pH was adjusted to pH=2 with concentrated HCl and the precipitated white solid was isolated by filtration and washed with cold distilled water (3×5 mL). Finally the product was dried to constant mass. Yield 1.78 g (52%). $^1$H NMR [360 MHz, $D_2O$] δ 4,05 (8H, s, $NCH_2$), 7,2-7,4 (4H, m, CHCH aromatic); $^{13}$C NMR [100 MHz, $D_2O$] δ 57,7 (4C $NCH_2$), 123,2(2C CH ring), 127,6 (2C CH ring), 141,0 (2C C ring), 174,7 (4C CO); MS (ESI) m/z 481,300 $(M+H)^+$ 35%; 503,282 $(M+Na)^+$ 100%; 519,250 $(M+K)^+$ 13%.

### Equilibrium studies

The $MnCl_2$, $CaCl_2$, $MgCl_2$, $ZnCl_2$ and $CuCl_2$ stock solutions were prepared from the highest analytical grade chemicals, and their concentrations were determined by complexometric titration with standardized $Na_2H_2EDTA$ and eriochrome black T indicator in the presence of ascorbic acid and potassium hydrogen tartrate for $MnCl_2$, murexide indicator for $CaCl_2$ and $CuCl_2$, eriochrome black T for $MgCl_2$ and xilenolorange in the presence of hexamethylenetetramine for the $ZnCl_2$ solution. The concentration of the ligand stock solution was determined by pH-potentiometric titrations. For determining the protonation constants of the ligand, pH potentiometric titrations were carried out with 0.2 M NaOH, using 0.002 M ligand solutions. The ionic strength was set to 0.15 M by using NaCl. The titrated samples (starting volume of 6 mL) were stirred mechanically and thermostated at 25 °C by a circulating water bath (±0.1 °C). The protonation constants of the ligand (log $K_i^H$) are defined as follows:

$$K_i^{H} = \frac{[H_iL]}{[H_{i-1}L][H^+]} \quad (3)$$

where $i$ = 1, 2, …, 5 and $[H_{i-1}L]$ and $[H^+]$ are the equilibrium concentrations of the ligand ($i$ = 1), protonated forms of the ligand ($i$ = 2, …, 5), and hydrogen ions respectively. To avoid the effect of $CO_2$, $N_2$ gas was bubbled through the solutions during the titrations process. The pH-potentiometric titrations were performed with a *Metrohm 785 DMP Titrino* titration workstation with the use of a *Metrohm 6.0234.100* combined electrode in the pH range of 1.8-12.0. For the calibration of the pH meter, KH-phtalate (pH = 4.005) and borax (pH = 9.177) buffers were used, and the $H^+$ concentrations were calculated from the measured pH values by applying the method proposed by Irving et al.[46] A solution of approximately 0.01 M HCl was titrated with a 0.2 M NaOH solution (0.15 M NaCl), and the differences between the measured and calculated pH values (for the samples with pH < 2.4) were used to calculate the $[H^+]$ from the pH values measured in the titration experiments. The measured points with pH > 11.0 of the acid-base titration were used to calculate the ionic product of water which was found to be 13.867 under our experimental conditions. For the calculation of the equilibrium constants, the PSEQUAD program was used.[47] The protonation constants of the PhDTA ligand were determined by titrating ligand solutions (acidified with a known volume of a standard HCl solution) with 0.2 M NaOH at 0.15 M ionic strength in the 1.8 – 12.0 pH range. The log $K_i^H$ values were calculated from 260 V(mL)-pH data pairs. The stability constants of the metal complexes were determined using the direct pH-potentiometric method by titrating samples with 1:1 and 2:1 metal-to-ligand ratios (the number of data pairs were between 150-200), allowing 1 min for the sample equilibration to occur. In the presence of metal excess the titration was continued until the appearance of the precipitate (pH = 7 – 9). The stability constant of the $Cu^{2+}$ complexes was too high to be determined by pH-potentiometry, hence a direct UV-vis spectrophotometric method was used. The spectrophotometric measurements were performed with a *Cary 100 Bio* spectrophotometer at 25 °C, using semimicro 1.0 cm cells. For the determination of the stability constant the absorbance was measured at 12 different acid concentrations (0.01 – 3.00 M) at 7 wavelengths between 650 and 800 nm (the concentration of the complex was 4.0 mM). A pH-titration of $[Cu(PhDTA)]^{2-}$ was also performed in the pH range 1.50-12.0 with a starting volume of 6 mL, $c_{Cu} = c_{PhDTA}$ = 2.0 mM.

**Kinetic Studies**

The dissociation rates of the $[Mn(PhDTA)]^{2-}$ complex were investigated at 25 °C and 0.15 M NaCl ionic strength by spectrophotometry, in the presence of a high (10-40-fold) excess of exchanging $Cu^{2+}$ ion to ensure pseudo-first-order conditions, using a *Cary 100 Bio* spectrophotometer at 300 nm (using semimicro 1.0 cm cells). The concentration of the complex was set to $2\times10^{-4}$ M, and the kinetic studies were performed by using a noncoordinating buffer, N'-methyl piperazine (NMP, log $K_2^H$ = 4.92(0.02)) at 0.04 M concentration to maintain constant pH in the samples. Before the kinetic runs only the solution of the complex was buffered, while in the solution of exchanging $Cu^{2+}$ the ionic strength was set. Under these conditions, the rate of the reaction can be expressed as follows: $-d[Mn(PhDTA)]^{2-}_{tot}/dt = k_{obs}[Mn(PhDTA)]^{2-}_{tot}$, where $k_{obs}$ is the pseudo-first-order rate constant and $[Mn(PhDTA)]^{2-}_{tot}$ is the total concentration of the $Mn^{2+}$ complex. The $k_{obs}$ values were determined using the following equation: $A_t = (A_r - A_p)e^{(-k_{obs}t)} + A_v$, where $A_t$ is the absorbance at time $t$, $A_r$ is the absorbance of the reactants, $A_p$ is the absorbance of the products.

**Determination of the relaxivity of the $Mn^{2+}$ Complex**

The relaxation times of water protons were measured at 20 MHz with a Bruker Minispec MQ-20 NMR Analyzer. The temperature of the sample holder was set to 25.0 ± 0.2 °C and controlled with the use of circulating water bath. The longitudinal relaxation times ($T_1$) were measured by using the inversion recovery method (180° – $\tau$ – 90°) by averaging 5-6 data points obtained at 8 different $\tau$ values. During the studies, the concentration of the $[Mn(PhDTA)]^{2-}$ complex was 1.0 mM ($I$ = 0.15 M NaCl) and the pH was varied in the range of 1.6 – 10.6.

**Cyclic voltammetry Experiments**

Cyclic voltammograms were recorded using a 797 VA Computrace potentiostat/galvanostat from Metrohm (Herisau, Switzerland) connected to a typical three electrode cell. A glassy carbon rotating disk electrode (stirring rate of 2000 rpms) was used as working electrode, while the counter electrode was a platinum rod. Potentials were measured using a Ag/AgCl reference electrode filled with 3 mol·$L^{-1}$ KCl. Solutions were purged with high purity (99.999%) nitrogen during 30 seconds prior recording the voltammograms. The starting and end potentials were 0.0 V, while the first vertex potential was set to +1.0 V. Sweep rates of 10 - 100 mV $s^{-1}$ were used.

**Computational Details**

The $[Mn(PhDTA)(H_2O)]^{2-}\cdot2H_2O$ and $[Mn(EDTA)(H_2O)]^{2-}\cdot2H_2O$ systems were fully optimized by using the hybrid GGA B3LYP[48] functional and the hybrid meta-GGA M062X[49] functional along with the TZVP[47] basis set. The nature of optimized geometries as true energy minima was confirmed by frequency analysis. Hyperfine coupling constants were calculated on the optimized structures by using the EPR-III basis set for the ligand atoms[51] and the aug-cc-pVTZ-J basis set for Mn.[52] Throughout this study bulk solvent effects were considered by using the integral equation formalism variant of the polarizable continuum model (IEFPCM).[53] All calculations were performed using the Gaussian 09 program package (revision D.01).[54]

## Acknowledgements

Authors are grateful for the support granted by the H Hungarian National Research, Development and Innovation Office (NKFIH K-120224 project) and for the János Bolyai Research Scholarship of the Hungarian Academy of Sciences (Gy.T. and K.F.K.). The research was also supported in a part by the EU and co-financed by the European Regional

Development Fund under the projects GINOP-2.3.2-15-2016-00008 and GINOP-2.3.3-15-2016-00004. Authors C. P.-I. and D. E.-G. thank Ministerio de Economía y Competitivad (CTQ2015-71211-REDT and CTQ2016-76756-P) and *Centro de Supercomputación de Galicia* (CESGA) for providing the computer facilities. This work was carried out within the frame of the COST CA15209 Action "European Network on NMR Relaxometry".

## Notes and references


1 É. Tóth, L. Helm and A. E. Merbach, In *The Chemistry of Contrast Agents in Medical Magnetic Resonance Imaging*, É. Tóth, A. E. Merbach, eds., Chichester: John Wiley & Sons, 2001.

2 (a) S. Cheng, L. Abramova, G. Saab, G. Turabelidze, P. Patel, M. Arduino, T. Hess, A. Kallen and M. Jhung, *J. Am. Med. Assoc.,* 2007, **297**, 1542. (b) T. H. Darrah, J. J. Prutsman-Pfeiffer, R. J. Poreda, M. E. Campbell, P. V. Hauschka and R. E. Hannigan, *Metallomics,* 2009, **1**, 479.

3 (a) B. Drahos, I. Lukes and E. Toth, *Eur. J. Inorg. Chem.* 2012, 1975. (b) M. Kueny-Stotz, A. Garofalo and D. Felder-Flesch, *Eur. J. Inorg. Chem.,* 2012, 1987. (c) D. Pan, A. H. Schmieder, S. A. Wickline and G. M. Lanza, *Tetrahedron,* 2011, **67**, 8431.

4 N. Kuznik and M. Wyskocka, *Eur. J. Inorg. Chem.,* 2016, 445.

5 P. B. Tsitovich, J. A. Spernyak and J. R. Morrow, *Angew. Chem. Int. Ed.,* 2013, **52**, 13997.

6 A. O. Olatunde, S. J. Dorazio, J. A. Spernyak and J. R. Morrow, *J. Am. Chem. Soc.,* 2012, **134**, 18503.

7 S. Aime, M. Botta, E. Gianolio, E. Terreno, *Angew. Chem. Int. Ed.,* 2000, **39**, 747.

8 G. L. Loving, S. Mukherjee and P. Caravan, *J. Am. Chem. Soc.,* 2013, **135**, 4620.

9 J. O. G. Karlsson, L. J. Ignarro, I. Lundstrom, P. Jynge and T. Almen, *Drug Discov. Today,* 2015, **20**, 411.

10 J. Crossgrove and W. Zheng, *NMR Biomed.,* 2004, 17, 544.

11 B. Drahos, V. Kubicek, C. S. Bonnet, P. Hermann, I. Lukes and E. Toth, *Dalton Trans.*, 2011, 40, 1945.

12 B. Drahos, M. Pniok, J. Havlickova, J. Kotek, I. Cisarová, P. Hermann, I. Lukes and É. Tóth, *Dalton Trans.,* 2011, 40, 10131.

13 A. de Sá, C. S. Bonnet, C. F. G. C. Geraldes, É. Tóth, P. M. T. Ferreira and J. P. Andre, *Dalton Trans.,* 2013, 42, 4522.

14 B. Drahos, J. Kotek, I. Cisarva, P. Hermann, L. Helm, I. Lukes and É. Tóth, *Inorg Chem.,* 2011, 50, 12785.

15 B. Drahos, J. Kotek, P. Hermann, I. Lukes and E. Tóth, *Inorg Chem.,* 2010, 49, 3224

16 Z. Garda, A. Forgacs, Q. N. Do, F. K. Kalman, S. Timari, Z. Baranyai, L. Tei, I. Toth, Z. Kovacs and G. Tircso, *J. Inorg. Biochem.,* 2016, **163**, 206.

17 A. Forgacs, L. Tei, Z. Baranyai, D. Esteban-Gomez, C. Platas-Iglesias and M. Botta, *Dalton Trans.,* 2017, **46**, 8494.

18 M. Khannam, T. Weyhermuller, U. Goswami and C. Mukherjee, *Dalton Trans.,* 2017, **46**, 10426.

19 A. Forgacs, R. Pujales-Paradela, M. Regueiro-Figueroa, L. Valencia, D. Esteban-Gomez, M. Botta and C. Platas-Iglesias, *Dalton Trans.,* 2017, **46**, 1546.

20 M. Regueiro-Figueroa, G. A. Rolla, D. Esteban-Gomez, A. de Blas, T. Rodriguez-Blas, M. Botta and C. Platas-Iglesias, *Chem. Eur. J.,* 2014, **20**, 17300.

21 J. S. Troughton, M. T. Greenfield, J. M. Greenwood, S. Dumas, A. J. Wiethoff, J. Wang, M. Spiller, T. J. McMurry and P. Caravan, *Inorg. Chem.,* 2004, **43**, 6313.

22 E. M. Gale, I. P. Atanasova, F. Blasi, I. Ay and P. Caravan, *J. Am. Chem. Soc.,* 2015, **137**, 15548.

23 F. K. Kálmán and Gy. Tircsó, *Inorg. Chem.*, 2012, **51**, 10065.

24 C. Vanasschen, M. Brandt, J. Ermert and H. H. Coenen, *Dalton Trans.,* 2016, **45**, 1315.

25 C. Vanasschen, E. Molnár, G. Tircsó, F. K. Kálmán, E. Tóth, M. Brandt, H. H. Cohen and B. Neumaier, *Inorg. Chem.,* 2017, **56**, 7746.

26 (a) W.Y. Ussov, M.L. Beljanin, O. Y. Borodin A. A. Churin A. I. Bezlepkin and V. D. Filimonov, Medical Visualization (in Russian), 2009, **5**, 121. (b) W. Y. Ussov A. A. Bogunetsky, V. E. Babokin, M. L. Belyanin, S. G. Goltsov and V. D. Filimonov, Tomsk/RU In ECR, 2014 March 6–10, 2014, Vienna, Austria; B-0904. (c) E. M. Gale, H.-Y. Wey, I. Ramsay, Y.-F. Yen, D. E. Sosnovik, P. Caravan, *Radiology,* 2018, *Epub ahead of print,* https://doi.org/10.1148/radiol.2017170977

27 E. Molnár, B. Váradi, Z. Garda, R. Botár, F. K. Kálmán, É. Tóth, C. Platas-Iglesias, I. Tóth, E. Brücher and Gy. Tircsó, *Inorg. Chim. Acta, 2018,* **472,** 254.

28 G. Liu, H. W. Dodgen and J. P. Hunt, *Inorg. Chem.,* 1977, **16**, 2652.

29 A. Mederos, J. M. Felipe, M. Hernandez-Padilla, F. Brito, E Chinea and K. Bazdikian, *J. Coord. Chem.*, 1986, **14**, 277.

30 E. Chinea, S. Domínguez, A. Mederos, F. Brito, J. M. Arrieta, A. Sánchez and G. Germain, *Inorg. Chem.*, 1995, **34**, 1579.

31 N. Nakasuka, M. Sawaragi, K. Matsumura, M Tana; *Bull. Chem. Soc. Jpn.,* 1992, **65,** 1722.

32 N. Nakasuka, M. Kunimatsu, K. Matsumura and M. Tanaka, *Inorg. Chem.,* 1985, **24**, 10.

33 T. Zhang, J.-M. Liu, X.-F. Huang, B. Xia, C.-Y. Su, G.-F. Luo, Y.-W. Xu, Y.-X. Wu, Z.-W. Mao and R.-L. Qiu, *J. Hazard. Mat.,* 2013, **262**, 464.

34 D. P. Riley, *Chem. Rev.*, 1999, **99**, 2573.

35 D. W. Margerum, J. B. Pausch, G. A. Nyssen and G. F., Smith, *Anal. Chem.,* 1969, **41***,* 233.

36 V. Patinec, G. A. Rolla, M. Botta, R. Tripier, D. Esteban-Gomez and C. Platas-Iglesias, *Inorg. Chem,* 2013, **52**, 11173.

37 N. Nakasuka, S. Azuma, C. Katayama, M. Honda, J. Tanaka and M. Tanaka, *Acta Cryst.,* 1985, C**41**, 1176.

38 E. M. Gale, J. Zhu and P. Caravan, *J. Am. Chem. Soc.,* 2013, **135**, 18600.

39 M. Regueiro-Figueroa, D. Esteban-Gomez, R. Pujales-Paradela, L. Caneda-Martinez, A. de Blas and C. Platas-Iglesias, *Int. J. Quantum Chem.,* 2016, **116**, 1388.

40 X. F. Wang, J. Gao, J. Wang, Zh. H. Zhang, Y. F. Wang, L. J. Chen, W. Sun, X. D. Zhang, Zh. Strukt. Khim. (Russ.) (J. Struct. Chem.) 2008, **49,** 753.


 

41 M. G. B. Drew, C. J. Harding, V. McKee, G. G. Morgan, J. Nelson, *J. Chem. Soc., Chem. Commun.,* 1995, **0,** 1035.
42 S. Durot, C. Policar, F. Cisnetti, F. Lambert, F., J.-P. Renault, G. Pelosi, G. Blain, H. Korri-Youssoufi, J.-P. Mahy, *Eur. J. Inorg. Chem.,* 2005, **17,** 3513.
43 J. Maigut, R. Meier, A. Zahl and R. van Eldik, *J. Am. Chem. Soc.*, 2008, **130**, 14556.
44 J. Maigut, R. Meier, A. Zahl and R. van Eldik, *Inorg. Chem.,* 2008, **47**, 5702.
45 G. Liu, H. W. Dodgen, J. P. Hunt, *Inorg. Chem.* 1977, **16,** 2652.
46 H. M. Irving, M. G. Miles and L. Pettit, *Anal. Chim. Acta*, **1967**, *38*, 475.
47 L. Zékány and I. Nagypál, In *Computational Methods for Determination of Formation Constants*; D. J. Legett, Ed., Plenum: New York, 1985, p 291.
48 (a) A. D. Becke, *J. Chem. Phys*., 1993, **98**, 5648. (b) C. Lee, W. Yang and R. G. Parr, *Phys. Rev. B,* 1988, **37**, 785.
49 Y. Zhao and D. G. Truhlar, *Theor. Chem. Accounts*, 2008, **120**, 215.
50 A. Schaefer, C. Huber and R. Ahlrichs, *J. Chem. Phys.,* 1994, **100**, 5829.
51 N. Rega, M. Cossi and V. Barone, *J. Chem. Phys.,* 1996, **105**, 11060.
52 E. D. Hedegard, J. Kongsted and S. P. A. Sauer, *J. Chem. Theory Comput.,* 2011, **7**, 4077.
53 J. Tomasi, B. Mennucci and R. Cammi, *Chem. Rev.,* 2005, **105**, 2999.
54 M. J. Frisch et al. Gaussian, Inc., Wallingford CT, 2009.